The Impact of Kinematic Redundancies on the Conditioning of a Planar Parallel Manipulator

J.V.C. Fontes, H.L. Vieira and M.M. da Silva

Department of Mechanical Engineering, São Carlos School of Engineering, University of São Paulo - USP, Brazil
e-mail: joao.fontes@usp.br, hiparcolins@usp.br, mairams@sc.usp.br

Abstract. Parallel manipulators present higher load capacity, better rigidity and other advantages when compared to the serial manipulators. However, parallel manipulators present drawbacks such as singularities inside their workspace and strongly coupled dynamics. In order to measure these drawbacks, the condition number of the Jacobian matrix can be used either as a measurement of the distance between the end effector and singularities or as an isotropy index. In this paper, a study of the impact of kinematic redundancies on the improvement of a planar manipulator's isotropicity and on the reduction of singularities is presented. In order to do so, conditioning maps are exploited for the non-redundant 3RRR and for the kinematically redundant 3PRRR manipulators. The outcome of this evaluation supports evidences in favor of kinematic redundancies regarding kinematic characteristics.

Key words: Parallel Kinematic Manipulator (PKM); Kinematic Redundancy; Singularity Avoidance; Conditioning Maps; Isotropy Index.

1 Introduction

Parallel kinematic manipulators (PKMs) can be promising industrial alternatives to serial manipulators due to their higher dynamic capabilities, higher accuracy and better payload/self-weight ratio [4]. Nevertheless, they present important drawbacks regarding real applications [5]. Some of these drawbacks are caused by the presence of singularities in the parallel manipulator's workspace. For instance, the accuracy of a PKM may rapidly decrease near singularities during a task. Kinematic redundancy can be applied to avoid or attenuate this problem. It consists in the introduction of an active joint in a kinematic chain allowing the self-motion of the manipulator. Due to the inclusion of the redundant actuator, the inverse kinematic model of kinematically redundant PKMs presents infinite solutions. A proper selection of a solution may enforce the avoidance of undesirable behaviour. In fact, kinematic redundancy has been used not only for the singularities' avoidance but also for the improvement of manipulator's kinematic and dynamic characteristics [2, 3, 6].

Additionally, PKMs present highly coupled dynamics which can become an issue for designing and implementing real-time control strategies for industrial applications [7]. The coupling of the mechanism can be measured by an isotropic index that can be defined by the condition number of the Jacobian matrix as described by [8]. This index is also exploited as a measurement of the distance between the end effector and singularities [1].

In this manuscript, a study of the impact of kinematic redundancies on the enhancement of the manipulator's isotropy and on the reduction of singular regions. This is accomplished by identifying the behaviour of the condition number of the Jacobian matrix of planar parallel kinematic manipulators with kinematic redundancy. In order to do that, the non-redundant manipulator, the 3RRR, and the kinematically redundant manipulator, the 3PRRR are investigated. These manipulators, illustrated in Fig. 1, present three kinematic chains composed of one active revolute joint (R) and two passive revolute joints (RR). The inclusion of extra active prismatic joints (P) is responsible for the kinematic redundancies.

The comparison of the behaviour of the condition number of the Jacobian matrix for predefined tasks could yield misleading interpretations, since this outcome is task dependent. In this way, conditioning maps are proposed and depicted over the manipulator's workspace. In this proposal, the kinematic redundancy is properly treated.

This paper is organized as follows. The kinematic model of the 3PRRR manipulator is described in Section 2. Section 3 presents the methodology addressing the conditioning maps. The results are presented and discussed in Section 4. Finally, conclusions are drawn in Section 5.

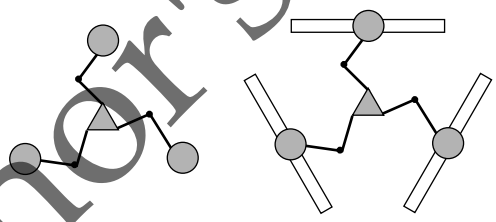

(a) (b)

Fig. 1 Illustrations of (a) the non-redundant manipulator 3RRR and (b) the kinematically redundant manipulator 3PRRR.

2 Kinematic Model

In this section, the kinematic model of the 3PRRR manipulator is presented. This model can be used to represent the non-redundant manipulator 3RRR by imposing

the input values of the redundant actuators. Figure 2 illustrates a scheme of the geometry of the 3PRRR. The subscript $i = 1, \ldots, 3$ describes the kinematic chain. There are revolute joints in A_i, B_i and C_i, where A_i is active and B_i and C_i are passive. The angles θ_i and β_i represent the orientation of the links A_iB_i and B_iC_i, respectively. The lengths of links A_iB_i and B_iC_i are, respectively, l_1 and l_2. Active prismatic joints can modify the position of the point A_i. Using this linear actuators the position of A_i can be modified according to the position δ_i and the orientation γ_i (see Fig. 2b). The distance between the manipulator's center and the central position of the linear actuators is represented by a. The Cartesian position of the end effector is (x, y) with orientation α. The distance of C_i to the center of the end effector is h. Details on this description can be found in [3].

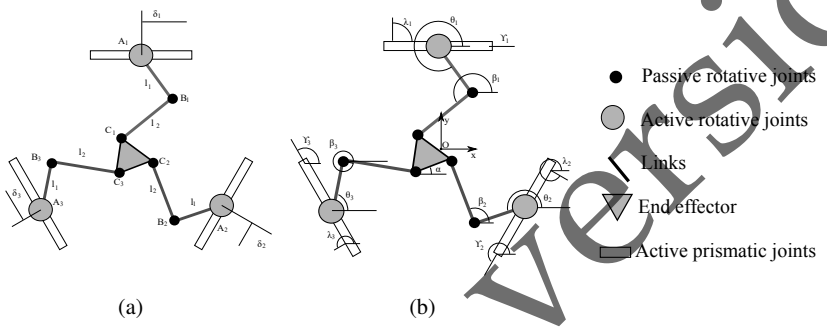

Fig. 2 Model parameters of the redundant manipulator 3PRRR: (a) Points and link lengths; (b) Angles and coordinate system.

2.1 Inverse Kinematics

The inverse kinematic model is used to determine the active joints' inputs $\Theta = [\theta_1, \theta_2, \theta_3, \delta_1, \delta_2, \delta_3]^T$ that yield a desired end effector's pose $\mathbf{X} = [x, y, \alpha]^T$. Due to the kinematic redundancies, this task is not simple since the mechanism presents six actuators while the end effector presents only three DOFs. As a consequence, this problem, usually denoted as redundancy resolution, presents infinite solutions. So, considering that the values of the redundant actuators' inputs δ_1, δ_2 and δ_3 are known, the inverse kinematics of the manipulator is defined.

First, the variables ρ_{xi} and ρ_{yi} are introduced as:

$$\begin{bmatrix} \rho_{xi} \\ \rho_{yi} \end{bmatrix} = \begin{bmatrix} x \\ y \end{bmatrix} + h \begin{bmatrix} cos(\alpha + \lambda_i) \\ sin(\alpha + \lambda_i) \end{bmatrix} - \delta_i \begin{bmatrix} cos(\gamma_i) \\ sin(\gamma_i) \end{bmatrix} - a \begin{bmatrix} cos(\lambda_i) \\ sin(\lambda_i) \end{bmatrix}. \quad (1)$$

The following geometrical constraint can be imposed according to the length of the links:

$$\left\| \begin{bmatrix} \rho_{xi} - l_1 cos(\theta_i) \\ \rho_{yi} - l_1 sin(\theta_i) \end{bmatrix} \right\| = l_2. \tag{2}$$

Expanding the norm in Eq. 2 and rearranging its result, the following relation can be obtained:

$$e_{i1} + e_{i2}\cos(\theta_i) + e_{i3}\sin(\theta_i) = 0, \tag{3}$$

where

$$e_{i1} = -2l_1\rho_{yi}, \tag{4}$$
$$e_{i2} = -2l_1\rho_{xi} \tag{5}$$
$$e_{i3} = \rho_{xi}^2 + \rho_{yi}^2 + l_1^2 - l_2^2 = 0. \tag{6}$$

The tangent half-angle substitution is employed to solve Eq. 3 for θ_i yielding:

$$\theta_i = 2\tan^{-1}\left(\frac{-e_{i1} \pm \sqrt{e_{i1}^2 + e_{i2}^2 - e_{i3}^2}}{e_{i3} - e_{i2}}\right). \tag{7}$$

Using Eq. 2 and the result of θ_i, the angle β_i can also be determined by

$$\beta_i = \tan^{-1}\left(\frac{\rho_{yi} - l_1\sin(\theta_i)}{\rho_{xi} - l_1\cos(\theta_i)}\right). \tag{8}$$

2.2 Jacobian Matrix

The Jacobian matrix $\mathbf{J}$, which relates $\dot{\mathbf{X}} = [\dot{x}, \dot{y}, \dot{\alpha}]^T$ with $\dot{\Theta} = [\dot{\theta}_1, \dot{\theta}_2, \dot{\theta}_3, \dot{\delta}_1, \dot{\delta}_2, \dot{\delta}_3]^T$, needs to be determined as well for the calculation of the manipulators' conditioning. This relation is defined as

$$\dot{\mathbf{X}} = \mathbf{J}\dot{\Theta} \tag{9}$$

One way to determine it is by taking the time derivative of the constraint relation described by Eq. 3. This approach yields:

$$\begin{aligned} \dot{x}[l_2\cos(\beta_i)] + \dot{y}[l_2\sin(\beta_i)] + \dot{\alpha}[l_2 h\sin(\beta_i - \lambda_i - \alpha)] = \\ = \dot{\theta}_i[l_1 l_2\sin(\beta_i - \theta_i)] + \dot{\delta}_i[l_2\cos(\beta_i - \gamma_i)]. \end{aligned} \tag{10}$$

Equation 10 can be rewritten in a matrix form yielding

$$\mathbf{A}\dot{\mathbf{X}} = \mathbf{B}\dot{\Theta}. \tag{11}$$

The matrices **A** and **B** can be defined as:

$$\mathbf{A} = \begin{bmatrix} a_{11} & a_{12} & a_{13} \\ a_{21} & a_{22} & a_{23} \\ a_{31} & a_{32} & a_{33} \end{bmatrix} \text{ and} \tag{12}$$

$$\mathbf{B} = \begin{bmatrix} b_{11} & 0 & 0 & b_{14} & 0 & 0 \\ 0 & b_{22} & 0 & 0 & b_{25} & 0 \\ 0 & 0 & b_{33} & 0 & 0 & b_{36} \end{bmatrix}. \tag{13}$$

where $a_{i1} = l_2\cos(\beta_i)$, $a_{i2} = l_2\sin(\beta_i)$, $a_{i3} = l_2 h\sin(\beta_i - \lambda_i - \alpha)$, $b_{ii} = l_1 l_2\sin(\beta_i - \theta_i)$ and $b_{ii+3} = l_2\cos(\beta_i - \gamma_i)$.

3 Conditioning map

The mathematical definition of singularities in PKMs is described by the determinant of the Jacobian matrices **A** and **B** [4]. Singular Jacobian matrices indicate singularities. Nevertheless, regions near to singularities can also be problematic for real applications and should be avoided. According to [1], the inverse of the condition number of the matrix **A** can be used to evaluate the closeness between the end effector and singularities.

From the kinematic model, one can notice that the matrix **A** is heterogeneous, thus its condition number has no physical meaning. This characteristic is due to the presence of translational and rotational DOFs. Therefore, in order to compensate and homogenize the matrix **A**, [1] have proposed a new homogenized matrix $\bar{\mathbf{A}}$ defined as:

$$\bar{\mathbf{A}} = \begin{bmatrix} a_{11} & a_{12} & a_{13}/Lc \\ a_{21} & a_{22} & a_{23}/Lc \\ a_{31} & a_{32} & a_{33}/Lc \end{bmatrix}, \tag{14}$$

where $Lc = \sqrt{2}h$ is the manipulator's characteristic length.

The condition number κ of the matrix $\bar{\mathbf{A}}$ can be defined as

$$\kappa(\bar{\mathbf{A}}) = \frac{max\ \sigma(\bar{\mathbf{A}})}{min\ \sigma(\bar{\mathbf{A}})}, \tag{15}$$

where $\sigma(\bar{\mathbf{A}})$ is the vector of singular values of the matrix $\bar{\mathbf{A}}$.

By definition, the index κ^{-1} is bounded, $(0 \leq \kappa^{-1} \leq 1)$. And, the following physical interpretation can be realized: $\kappa^{-1} = 0$ means that the manipulator is on a singularity and $\kappa^{-1} = 1$ means that it is on an ideal isotropic configuration. In this way, [1] have demonstrated that the index κ^{-1} indicates the distance between the end effector and the singularities.

Since the index κ^{-1} is dependent on the manipulators' configuration, its value is not constant over the manipulators' workspace. In this way, the values of the index κ^{-1} can be calculated in a mesh over the manipulator's workspace. Conditioning maps can be depicted by plotting these values over the workspace.

For non-redundant manipulator, the 3RRR manipulator, a single kinematic configuration is derived by the inverse kinematic model. In this way, a single value of the index κ^{-1} is found for each configuration defined by the mesh. For the kinematically redundant manipulator, the 3PRRR manipulator, infinite configurations can be derived for a single pose of the end effector. In this work, the conditioning map for the redundant manipulator is derived by dividing each input of the active prismatic joints (the redundant actuators, δ_i) in k possible positions. The best inputs are found by extensive search for the higher value of the index κ^{-1}. The higher values of the index κ^{-1} are depicted yielding the conditioning maps for the redundant case.

4 Results

In this comparison, the parameters for both manipulator are the same. Moreover, these values have been selected in order to match a real setup built by our research group [9]. The lengths of each link l_1 and l_2 are 0.191 m and 0.232 m, respectively. The limits of the linear actuators are $\delta_{min} = -0.3$ m and $\delta_{max} = 0.3$ m. The lengths a_i and h_i are the same for all kinematic chains and are equal to 0.260 m and 0.060 m, respectively.

Figure 3 depicts the conditioning map of the 3RRR manipulator. There are three unreachable circles inside the workspace due to the difference in the lengths of links l_1 and l_2. Moreover, the dark blue areas near to these circles present low condition numbers. This indicates that these regions are close to singularities. In general, the conditioning map of the 3RRR shows that the manipulator conditioning is lower than 0.8 in a large amount of the workspace. Conditioning values higher than 0.8 can only be found at regions near to the center of the workspace.

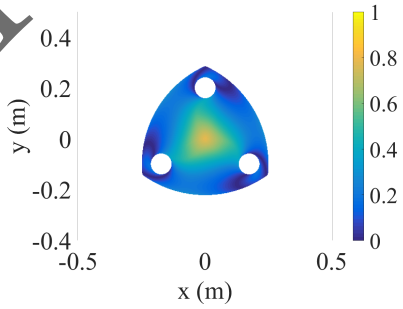

Fig. 3 Conditioning map of the non-redundant manipulator 3RRR.

Figure 4 illustrates the conditioning map of the 3PRRR manipulator. One can notice that there is no unreachable area inside the workspace, which is considerable larger than the 3RRR's workspace. Moreover, there is no area that presents a conditioning index lower than 0.2 and there is a wide area with conditioning index higher than 0.8 in the center of the workspace.

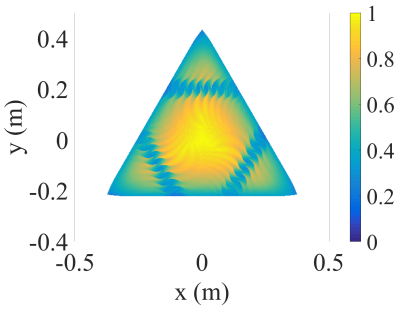

Fig. 4 Conditioning map of the redundant manipulator 3PRRR.

Comparing Figs. 3 and 4, one can notice that the region with index values higher than 0.8 (yellow area) presents the same size of the 3RRR workspace. This suggests that kinematic redundancy promotes the improvement of the manipulator's conditioning, since the 3PRRR manipulator generally presents higher conditioning values than the 3RRR manipulator.

Although the redundant manipulator has shown a better conditioning map, these aforementioned values can only be achieved in specific inputs of the active prismatic joints (the redundant actuators 1, 2 and 3). These optimal inputs are depicted in the workspace in Figs. 5(a), 5(b) and 5(c). One can observe that there are some important discontinuities regions in these maps leading to unfeasible trajectories for the redundant actuators. Indeed, this fact shows that the proposal of a strategy to design smooth optimal position maps can be helpful for the design of redundant manipulators. These maps can be useful for deriving redundancy resolution scheme for real applications.

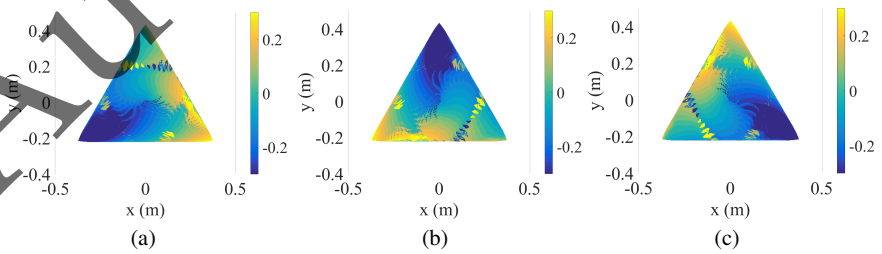

Fig. 5 Optimal inputs for the redundant actuators (a) δ_1, (b) δ_1 and (c) δ_1.

5 Conclusions

In general, PKMs present high coupled dynamics and singularities in the workspace. In order to avoid these drawbacks, kinematic redundancy can be applied as stated in the literature. In this manuscript, the impact of kinematic redundancy on the conditioning of PKMs was addressed. In order to do that, two manipulators were compared: the non-redundant 3RRR and the redundant 3PRRR manipulators. This comparison was carried out by contrasting the conditioning maps of both manipulators. These maps were depicted by plotting the inverse of the condition number of the homogenized Jacobian matrix in the manipulator's workspace.

The results demonstrated a considerable increase in the area where the conditioning index is larger than 0.8 when kinematic redundancies are considered. This indicates that kinematic redundancies can be an alternative for improving the performance of PKMs. Finally, the authors believe that these conditioning maps could be applied to the development of a redundancy resolution scheme improving the conditioning of redundant manipulators for real applications.

Acknowledgements This research is supported by FAPESP 2014/01809-0, FP7-ITN Grant Agreement 315967 - EMVeM (Energy Efficiency Management for Vehicles and Machines) and CNPq.

References

1. Alba-Gomez, O., Wenger, P., Pamanes, A.: Consistent Kinetostatic Indices for Planar 3-DOF Parallel Manipulators, Application to the Optimal Kinematic Inversion. In: Volume 7: 29th Mechanisms and Robotics Conference, Parts A and B, vol. 2005, pp. 765–774. ASME (2005). DOI 10.1115/DETC2005-84326
2. Do Thanh, T., Kotlarski, J., Heimann, B., Ortmaier, T.: Dynamics identification of kinematically redundant parallel robots using the direct search method. Mechanism and Machine Theory **55**, 104–121 (2012). DOI 10.1016/j.mechmachtheory.2012.03.011
3. Fontes, J.V., da Silva, M.M.: On the dynamic performance of parallel kinematic manipulators with actuation and kinematic redundancies. Mechanism and Machine Theory **103**, 148–166 (2016). DOI 10.1016/j.mechmachtheory.2016.05.004
4. Gosselin, C., Angeles, J.: Singularity analysis of closed-loop kinematic chains. IEEE Transactions on Robotics and Automation **6**(3), 281–290 (1990). DOI 10.1109/70.56660
5. Merlet, J.P.: Parallel Robots. Springer (2006)
6. Mohamed, M.G., Gosselin, C.M.: Design and analysis of kinematically redundant parallel manipulators with configurable platforms. Robotics, IEEE Transactions on **21**(3), 277–287 (2005). DOI 10.1109/TRO.2004.837234
7. Paccot, F., Andreff, N., Martinet, P.: A Review on the Dynamic Control of Parallel Kinematic Machines: Theory and Experiments. The International Journal of Robotics Research **28**(3), 395–416 (2009). DOI 10.1177/0278364908096236
8. Patel, S., Sobh, T.: Manipulator Performance Measures - A Comprehensive Literature Survey. Journal of Intelligent & Robotic Systems **77**(3-4), 547–570 (2015). DOI 10.1007/s10846-014-0024-y
9. Santos, J.C., Frederice, D., Fontes, J.V.C., da Silva, M.M.: Numerical Analysis and Prototyping Details of a Planar Parallel Redundant Manipulator. In: 2015 12th Latin American Robotics Symposium and 2015 3rd Brazilian Symposium on Robotics (LARS-SBR), pp. 55–60. IEEE, IEEE (2015). DOI 10.1109/LARS-SBR.2015.30